

# Physical Characterization of Gap Junction Membrane Connexons (Hemi-channels) Isolated from Rat Liver\*

(Received for publication, February 21, 1995, and in revised form, May 1, 1995)

Michael Cascio‡, Nalin M. Kumar§, Robert Safarik, and Norton B. Gilula

From the Department of Cell Biology, The Scripps Research Institute, La Jolla, California 92037 and the ‡Department of Molecular Genetics and Biochemistry, University of Pittsburgh School of Medicine, Pittsburgh, Pennsylvania 15261

**Enriched subcellular fractions of double membrane gap junctions (plaques) from rat livers were treated under reducing conditions with high salt and non-ionic detergent concentrations at high pH to obtain a preparation of structural 80–90 Å complexes of oligomers (connexons). The isolated oligomers were chromatographically purified, and subsequently characterized immunologically, morphologically by electron microscopy, hydrodynamically by gel filtration and ultracentrifugation, spectroscopically by circular dichroism, and chemically via cross-linking studies. The physical characteristics of these isolated gap junction complexes were compared to those of native membrane-bound gap junctions in rat liver. These analyses indicate that the isolated complex (connexon) principally contains a hexameric arrangement of gap junction protein to form a single membrane hemi-channel.**

Paired protein channels located in specialized areas of closely apposed plasma membranes, termed gap junctions, act to connect the interiors of adjacent cells in a tissue. These channels allow for direct intercellular communication between cells by acting as a conduit for the passage of ions and small molecules, and they are important for the regulation of development and cell growth (for reviews, see Refs. 1, 2). It is now recognized that a family of gap junction proteins exists, members of which are expressed differentially in virtually all cell types (3, 4).

This study has focused on the gap junction channel of rat livers which is comprised primarily of a single 32-kDa protein component (5–7), with less than 5% of the gap junction protein being a related 26-kDa protein species (8). The mRNAs for both proteins have been cloned and sequenced (9–11). These are referred to as  $\beta_1$  (or Cx32) and  $\beta_2$  (or Cx26) gap junction proteins.

Electrophoretically eluted (from SDS-polyacrylamide gels) rat liver  $\beta_1$  protein has been reported to form voltage-dependent channels in reconstituted lipid bilayers (12), and the topology of the molecule has been partially mapped (13–16). Upon isolation and purification, hepatic gap junction proteins form extended two-dimensional crystalline arrays. Low resolution three-dimensional structural information has been obtained from electron micrographs of tilted specimens (17–19) and low angle x-ray diffraction studies of stacked arrays (20, 21). These studies have suggested that each channel is composed of two hexameric assemblies which span the opposing membranes

and meet at the center of the gap. Additionally, the secondary structure of the rat liver gap junction channel in sonicated membrane patches has been determined by circular dichroism (CD) studies (22). Unfortunately, the presence of the membrane bilayer in which the oligomers are embedded has precluded structural examination of the oligomer at a molecular level. Conditions have been described (19) under which the  $\beta_1$  connexin protein may be solubilized by detergent while retaining a native-like structure.

Using conditions similar to those described by Stauffer *et al.* (19), we have isolated and purified the rat liver  $\beta_1$  gap junction protein in a “native” oligomeric state. These isolated complexes were, in turn, characterized to determine the physical properties of the oligomeric unit.

## EXPERIMENTAL PROCEDURES

**Materials**—Female retired breeder Sprague-Dawley rats, ranging from 200 to 300 g were obtained from Holtzman Laboratories (Madison, WI). *N,N*-Dimethyldodecylamine-*N*-oxide (LDAO)<sup>1</sup> was purchased from Fluka (Switzerland). Dodecyl maltoside and dithiothreitol (DTT) were purchased from Calbiochem (San Diego, CA). Tris, HEPES, and triethanolamine (TEA) were purchased from Sigma. EDTA was purchased from Fisher.

**Specimen Preparation**—Subcellular fractions of enriched rat liver gap junctions were prepared by alkali-extraction (NaOH) of rat liver plasma membrane fractions according to Hertzberg (7), as modified by Zimmer *et al.* (13). The isolated gap junction fractions were stored in 2 mM bicarbonate buffer, pH 7.5, at  $-70^\circ\text{C}$ .

**Gel Filtration**—Gel filtration was carried out on a Waters 510 HPLC system equipped with an LKB Uvicord SII model 2238 detector and a 277-nm filter. Separations were performed at 0.5 ml/min on a 7.5 × 300 mm TSK G3000SW column with a 7.5 × 75 mm TSK SWP pre-column (Toyo Soda, Japan) by isocratic elution with 1 M NaCl, 20 mM Tris, pH 7.2, 5 mM DTT, and 0.05% LDAO.

Markers used in the Stokes radius determination were horse heart myoglobin (Sigma), bovine heart malate dehydrogenase (Sigma), bovine heart lactate dehydrogenase (Sigma), horse spleen ferritin (Gallard Schlesinger),  $\beta$ -galactosidase (Worthington Biochemicals), and blue dextran (Sigma).

Isolated gap junctions were solubilized by resuspension of the pellet (15 min at  $12,000 \times g$  at  $4^\circ\text{C}$ ) in 0.4% LDAO, 2 M NaCl, 10 mM Tris, pH 9.4, and 10 mM DTT at a final concentration of 1 mg/ml. The suspension was vortexed for at least 2 h at  $4^\circ\text{C}$ . The sample was then diluted with an equal volume of 100 mM Tris at pH 7.2. Particulates were pelleted as before, and 200  $\mu\text{l}$  of the supernatant was injected onto the column. In this paper, the non-pelleting material in the presence of detergent will be referred to as gap junction complexes or oligomers.

Larger scale separations ( $>500 \mu\text{g}$ ) were conducted on a Pharmacia FPLC system equipped with a P-500 pump and a UV-1 monitor with a 280-nm filter using a Superose 6 HR 10/30 column (Pharmacia). Samples were prepared as above except the sample was solubilized in 100 mM glycine, pH 10.0, 2 M NaCl, 100 mM DTT, 10 mM EDTA, and 2.0% LDAO to give a final concentration of  $\sim 0.5$  mg/ml, and then concentrated 2–3-fold using a Centricon 10 microconcentrator (Amicon,

\* This work was supported by NIH Grant GM 37904 to N.B. Gilula, EY 06884 to N. Kumar, and GM 41449 to N. Unwin. The costs of publication of this article were defrayed in part by the payment of page charges. This article must therefore be hereby marked “advertisement” in accordance with 18 U.S.C. Section 1734 solely to indicate this fact.

§ To whom correspondence should be addressed: Dept. of Cell Biology, The Scripps Research Institute, 10666 N. Torrey Pines Rd., MB6, La Jolla, CA 92037. Tel. 619-554-4236; Fax: 619-554-6945.

<sup>1</sup> The abbreviations used are: LDAO, *N,N*-dimethyldodecylamine-*N*-oxide; DTT, dithiothreitol; TEA, triethanolamine; HPLC, high performance liquid chromatography; FPLC, fast performance liquid chromatography; NRMSD, normalized root mean standard deviation; PAGE, polyacrylamide gel electrophoresis; DMS, dimethyl sulfoxide.

Danver, MA). A 1.0-ml aliquot was injected onto the column, using a running buffer consisting of 50 mM HEPES, pH 8.0, 1.0 M NaCl, 10 mM DTT, 10 mM EDTA, and 0.5% LDAO at a flow rate of 0.5 ml/min.

Eluent of HPLC and FPLC were monitored for gap junction content by electron microscopy, SDS-PAGE, and/or immunoblotting.

**Ultracentrifugation**—Linear 2-ml 5–20% or 10–25% sucrose gradients (Schwarz/Mann UltraPure grade) in H<sub>2</sub>O or D<sub>2</sub>O in 20 mM Tris, pH 9.2, 1 M NaCl, 5 mM DTT, and 0.05% LDAO were generated by freezing and thawing a gradient containing five steps of sucrose. Marker proteins or solubilized gap junction samples (separated by HPLC or FPLC) were applied to the top of the gradients. All marker proteins were purchased from Sigma, and their respective partial specific volumes and corrected sedimentation coefficients were: horse heart myoglobin, 0.741 ml/g and 2.04 s, chicken egg ovalbumin, 0.744 ml/g and 3.53 s, bovine transferrin, 0.725 ml/g and 4.92 s, rabbit muscle aldolase, 0.735 ml/g and 7.35 s, and bovine liver catalase, 0.730 ml/g and 11.30 s (23). Gradients were centrifuged at 55,000 for 4 h at 4°C (no brake) in a TL555 swinging bucket rotor in a TL100 ultracentrifuge (Beckman Instruments). Gradients were fractionated by piercing with a 25-gauge needle. The refractive indices of the fractions were determined with an Atago R5000 hand refractometer. The sedimentation of the markers was determined by SDS-PAGE and the presence of gap junction complexes by electron microscopy.

**SDS-PAGE**—Preparations were analyzed by SDS-PAGE according to Laemmli (24), but without boiling. Bands were visualized by Coomassie (Brilliant) Blue or silver staining (13).

**Immunoblotting**—Affinity-purified antibodies prepared against synthetic peptides corresponding to proposed cytoplasmic loops of the human  $\beta_1$  liver protein (14) and the rat  $\beta_2$  liver protein (25) were used for immunoblotting. These antibodies were prepared, purified, and characterized as described previously (14). Western transfers were conducted using a modification of the procedure of Towbin *et al.* (26), as described by Milks *et al.* (14). Antibody binding was detected by <sup>125</sup>I-protein A and visualized by autoradiography. Where noted, band intensities were digitized with an LKB Ultrosan XL laser densitometer.

**Electron Microscopy**—Acetone-washed 400 mesh copper grids (Ernest Fullam Co.) were coated with 5% collodion in amyl acetate (Ted Pella, Inc.) and stabilized with a carbon film using an Edwards E306A Coating System. The collodion was then removed with acetone, and the grids glow-discharged using an EMScope model 350 unit. Samples were applied to the grids for 1 min and then blot dried using filter paper applied to the grid edge. Each grid was washed three times by inversion onto a drop of 10 mM Tris-buffered solution, pH 9.2, for 1 min, with blotting between washes, and stained by inverting on a drop of 1% uranyl acetate solution for 1–2 min and blot-dried. Samples were examined on a Philips CM-12 electron microscope at 100 kV.

**Circular Dichroism Spectroscopy**—Native double-membrane junctions were pelleted as before, resuspended in 10 mM Tris, pH 9.2, and sonicated to clarity with a Branson Sonifier microprobe using repeated 8–12-s bursts. During this procedure, the sample vial was placed in an ice water-jacketed chamber to prevent heating. Typically, five bursts were sufficient to render the solution transparent. The membrane suspensions were centrifuged at 12,800  $\times g$  for 15 min and the supernatant containing the smaller membranes fragments used for further analysis.

The isolated gap junction oligomers were purified by FPLC prior to CD examination. The samples were dialyzed against 10 mM Tris, pH 9.2, 125 mM NaCl, 5 mM DTT, and 0.05% LDAO and concentrated using an Amicon microconcentrator and characterized as above. Aliquots of the dialysate were used as blanks.

CD spectra were recorded on an Aviv 61DS spectropolarimeter. The spectropolarimeter was calibrated for wavelength using benzene vapor. The optical rotation was calibrated with D-10-camphorsulfonic acid and checked with sperm whale myoglobin.

Optical measurements of ellipticity were routinely made at room temperature using a demountable quartz cell (Hellma Kuvetten, Mullheim/Baden, Germany) of pathlength 0.5 mm for the junctions and 0.1 mm for the isolated oligomers. Data was collected at 0.2-nm intervals in the wavelength range between 300 and 185 nm for the former, and between 300 and 195.4 nm for the latter (the presence of high salt, DTT, and LDAO in the solubilization buffer precluded collection at lower wavelengths). At least 15 reproducible scans were collected for each sample, averaged, and then smoothed using a Savitzky-Golay filter (27).

The CD spectra were analyzed in the wavelength range from 190 to 240 nm using a non-linear least-squares curve-fitting procedure, with the values of the fractions of secondary structure constrained to be non-negative and normalized, as described previously (28). The reference data set (29) was augmented with a basement membrane collagen data set (22) to correct for any collagen content. A helix length of 20

residues, the minimum length of helix necessary to span the lipid bilayer, was used in all analyses. The quality of the fit of the reference spectra to the experimental data was evaluated by calculating a fit parameter, the normalized root mean standard deviation (NRMSD) (28).

The spectrum of a polypeptide in the near UV region is a sum of the individual absorbances of three peptide transitions in this region: a single  $n$  to  $\pi^*$ , and two  $\pi$  to  $\pi^*$  transitions, one parallel and one perpendicular to the optical beam. Since the energy, and thus the location of the absorption peak, of each transition dipole is affected by the dipole moment of its local environment, the CD bands of the various peptide transitions of membrane proteins may be differentially red- or blue-shifted relative to their location in the spectrum of an aqueous protein (30). Accordingly, additional analyses were conducted in which the reference basis sets were deconvoluted to yield three gaussian absorption bands, and these bands shifted independently to optimize the fit of the reference data base to the experimental spectrum as reflected by minimization of the NRMSD (22, 31, 32). The calculated secondary structures determined by this type of analysis may reflect the actual secondary structure present more accurately and are included in the calculations as a limit for the variability in our calculations of net protein conformation.

**Cross-linking**—Gap junction membranes were solubilized in 2% Dodecyl maltoside, 20 mM TEA, pH 9.2, 20 mM EDTA, and 10 mM DTT, at a concentration of 0.5 mg/ml. To cross-link, a 100 mM DMS (Pierce) stock solution in 200 mM TEA, pH 9.2, was diluted 10-fold in the buffer and allowed to react at 4°C. The reaction was quenched at various time points with excess glycine. Reaction products were analyzed by immunoblotting.

## RESULTS

**Preparation of the Isolated Gap Junction Oligomers**—Conditions for dissociating the isolated gap junction membranes into oligomeric units were adapted from Stauffer *et al.* (19), using LDAO as the detergent. Oligomers were then isolated by gel filtration on either HPLC or FPLC systems. Buffer conditions were slightly different for HPLC and FPLC since restrictions due to the chemical nature of the silica matrix of the HPLC column required the sample pH to be reduced before chromatography on this system. The elution volume,  $V_e$ , of gap junction complexes isolated under these conditions was determined by examining electron micrographs of negatively stained aliquots of the eluant. Aliquots containing gap junction oligomers were identified by the appearance of 70–80 Å circular structures containing a central 15–20-Å electron-dense center (*i.e.* 70–80 Å diameter “doughnuts”) (Fig. 1B); structures which are similar to those observed in electron micrographs of isolated gap junction plaques (Fig. 1A). The presence of  $\beta_1$  protein in these samples was confirmed by immunoblotting. Immunoblots indicated that  $\beta_2$  protein was present also in the samples before injection (but, relative to  $\beta_1$  protein, at much lower concentrations). This protein was also detected in the FPLC eluant but not in the HPLC eluant. The  $\beta_2$  protein was observed to co-elute with  $\beta_1$  protein (Fig. 2). The absence of detectable  $\beta_2$  protein in the HPLC eluant was probably due to less material being loaded on the HPLC column resulting in dilution below the detection limit during chromatography.

**Stokes Radius ( $R_s$ ) Determination**—Size information of the gap junction complex isolated in detergent was obtained by gel filtration on HPLC in three independent experiments. The partition coefficient,  $K_d$ , of a species is defined as (33):

$$K_d = (V_e - V_o)/(V_i - V_o) \quad (\text{Eq. 1})$$

where  $V_o$  is the void volume of the column and  $V_i$  is the total volume of the column. In these studies, the  $V_o$  was  $5.77 \pm 0.15$  ml as measured with blue dextran, and the  $V_i$  was  $18.19 \pm 0.65$  ml by salt elution. Le Maire *et al.* (34) have shown that for HPLC gels in general, and TSK3000 SW columns in particular, the porous media of the gel may best be described as surface fractals, and there exists a linear relationship between  $\ln R_s$  and  $\ln (1 - K_d)$ . By measuring the  $V_e$  (by  $A_{277}$ ) of various marker proteins of known  $R_s$ , the gap junction complex was

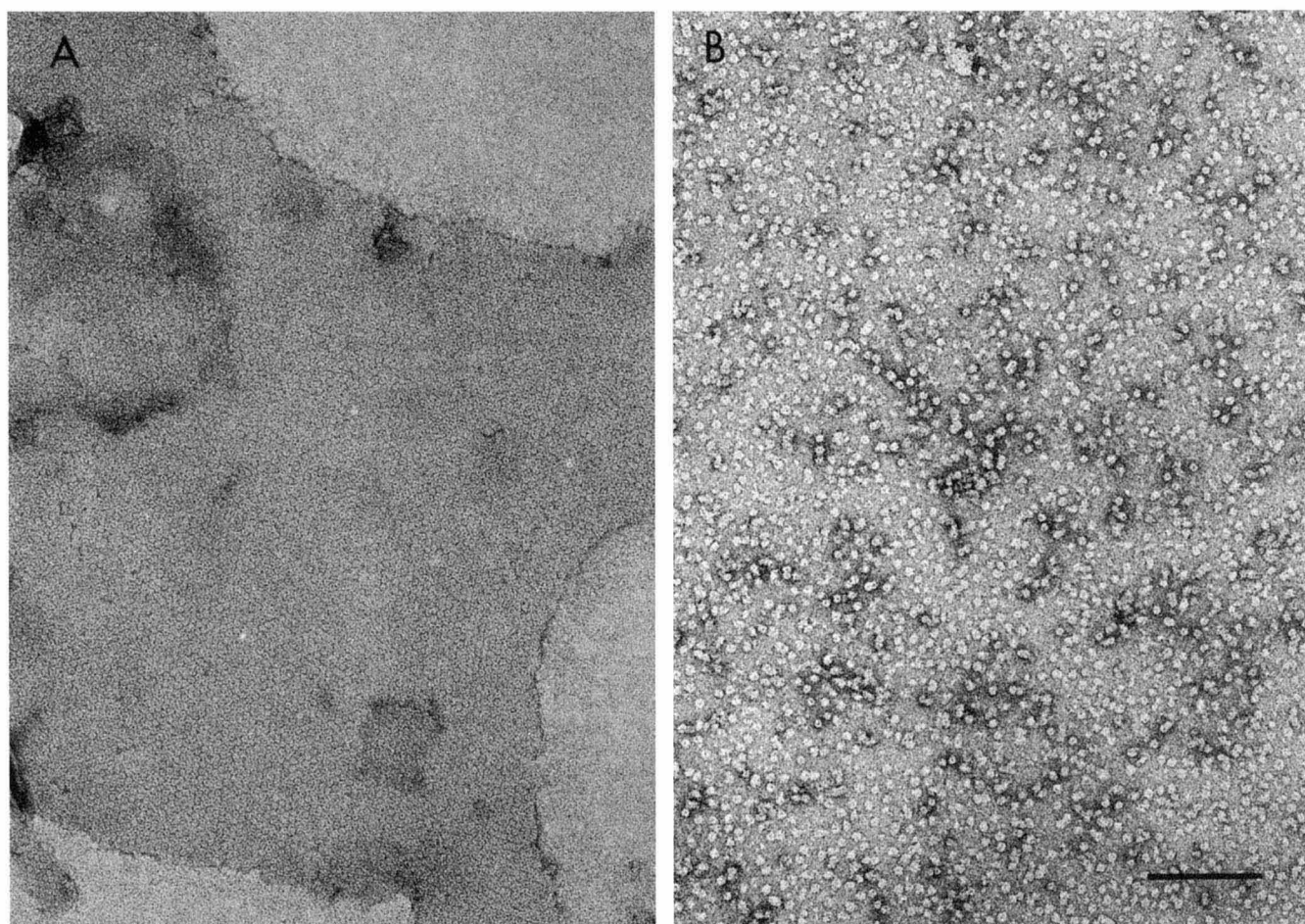


FIG. 1. **Electron micrographs of gap junction preparations.** Negatively stained images of gap junction-enriched plaques isolated from rat liver tissue (A), and detergent-solubilized preparations isolated after gel filtration (B). These isolated protein-detergent complexes had physical characteristics consistent with hexameric assemblies. The bar represents 200 nm.

determined to have an  $R_s$  of  $41.0 \pm 0.6$  Å (Fig. 3).

**Determination of  $s_{20,w}$  and Molecular Weight**—The sedimentation coefficient,  $s$ , and partial specific volume,  $\nu$ , of the isolated complex was determined by using markers of known  $\nu$  and  $s_{20,w}$  in ultracentrifugation experiments on parallel linear gradients in  $H_2O$  and  $D_2O$  (35, 36). The composition of the fractions was determined by SDS-PAGE of the markers and by electron microscopy, and confirmed by immunoblotting, as described above, for the solubilized gap junctions. It was assumed that detergent binding is equivalent in  $H_2O$  and  $D_2O$ ; this assumption results in less than 10% error in the calculated molecular weight of other membrane proteins (35). The similarity of the  $s_{20,w}$  calculated from  $H_2O$  and  $D_2O$  gradients (8.76 and 8.74 s, respectively) indicate that this is a valid assumption. The sedimentation coefficients for the markers and the gap junctions were determined by measuring the half-distance of migration,  $r_{avg}$ , and from the relationship:

$$s_{T,m(avg)} = (r - r_o)/\omega^2 r_{avg} t \quad (\text{Eq. 2})$$

The linearity of the gradients was confirmed by measurement of the refractive indices of the fractions. The density,  $\rho$ , at any point in the gradient was determined by interpolation of the measured density at the top and bottom of the gradients. The average viscosity,  $\eta$ , experienced by the marker proteins, was determined from the relationship:

$$\eta_{T,m(avg)} = (s_{20,w}/s_{T,m})(1 - \nu\rho_{T,m(avg)})/(1 - \nu\rho_{20,w}) \quad (\text{Eq. 3})$$

The average viscosity experienced by the gap junction complex in each gradient was interpolated from linear plots of  $\eta_{avg}$

for the markers *versus* gradient fraction. The partial specific volume of the complex,  $\nu$ , can then be calculated:

$$\nu = (s_H\eta_H/s_D\eta_D - 1)/(\rho_{D(avg)}(s_H\eta_H/s_D\eta_D) - \rho_{H(avg)}) \quad (\text{Eq. 4})$$

and is reported in Table I. The sedimentation coefficient corrected to water at 20 °C was then determined from both the  $H_2O$  and  $D_2O$  gradients since:

$$s_{20,w} = s_m(\eta_m/\eta_{20,w})(1 - \nu\rho_{20,w})/(1 - \nu\rho_H) \quad (\text{Eq. 5})$$

These values are reported in Table I.

Using this information, along with the calculated  $R_s$  from gel filtration, we can then determine the molecular weight of the complex:

$$M_r = s_{20,w} \eta_{20,w} 6 \pi N R_s / (1 - \nu\rho_{20,w}) \quad (\text{Eq. 6})$$

and the frictional ratio from:

$$f/f_0 = R_s(4 \pi N/3 M_r \nu)^{1/3} \quad (\text{Eq. 7})$$

These values are reported in Table I.

To determine the molecular weight of the protein alone, we can use the relationship that

$$\nu_{complex} = \nu_P f_P + \nu_D f_D \quad (\text{Eq. 8})$$

where  $f_P$  and  $f_D$  are the fractional weight composition of protein and detergent, respectively;  $\nu$  for LDAO is 1.112 ml/g and  $\nu_P$  was calculated from the amino acid composition to be 0.748 ml/g (37).

**CD Spectroscopy**—The secondary structures of the isolated gap junction oligomers and the gap junction membranes may

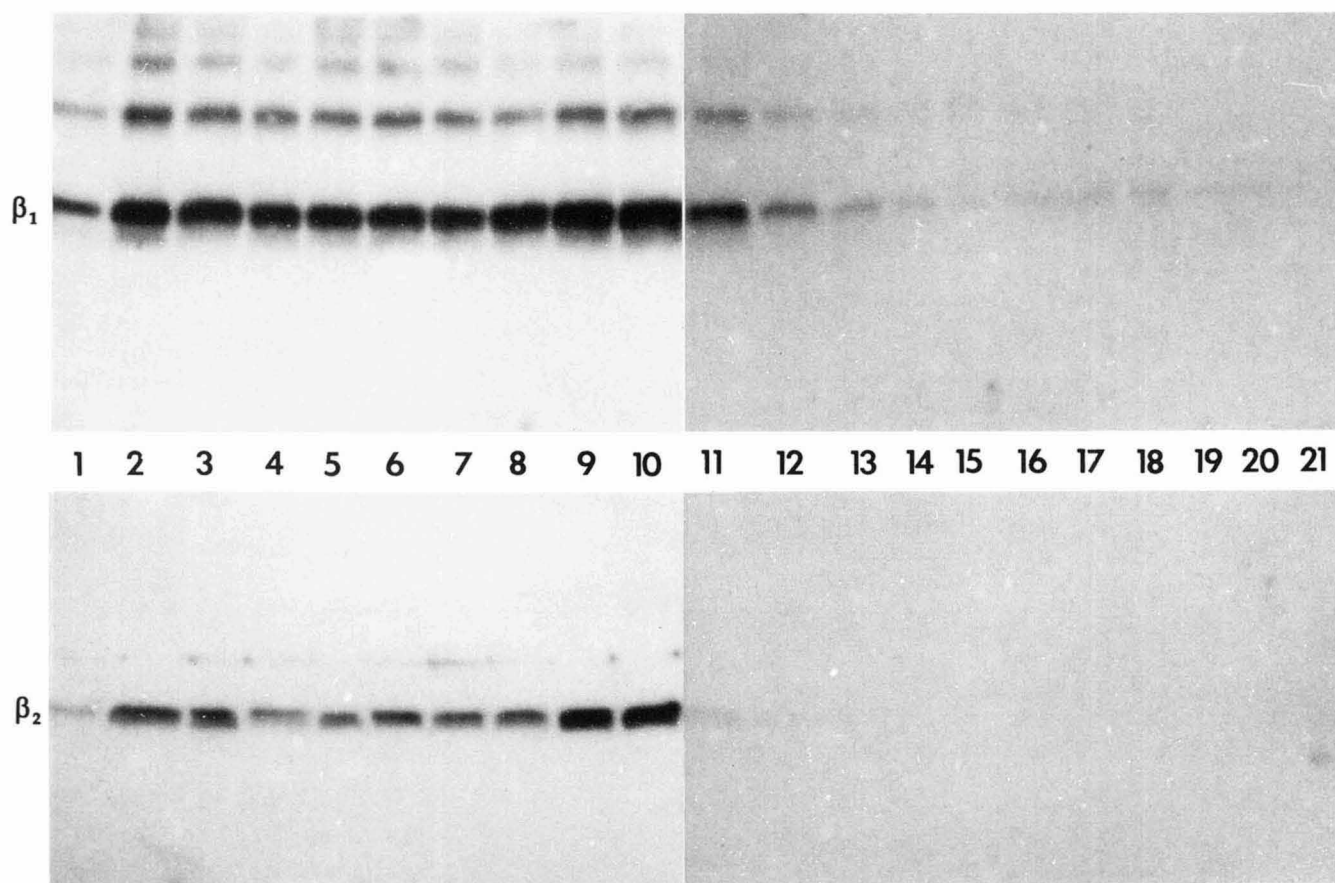


FIG. 2. Immunoblots of fractions from gel filtration of detergent-solubilized gap junctions. 1–1.5 mg of protein were applied to a Superose 6 HR 10/30 column and eluted at 0.5 ml/min. Fractions were run on a 15% SDS-polyacrylamide gel and transferred to nitrocellulose. Immunoblots were treated with antibodies to  $\beta_1$  liver connexins or  $\beta_2$  liver connexins. The position of the monomers of  $\beta_1$  and  $\beta_2$  gap junction protein is indicated on the left-hand side.

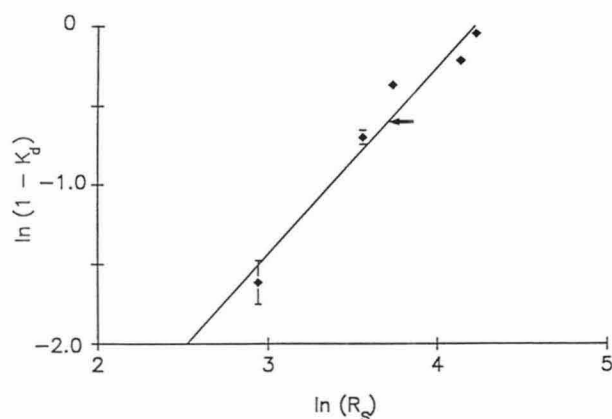


FIG. 3. Plot of  $\ln R_s$  versus  $\ln (1 - K_d)$  as determined by gel filtration on a TSK3000 SW column. The marker proteins used with their corresponding  $R_s$  values (in Å) were myoglobin, 18.9, malate dehydrogenase, 35.1, lactate dehydrogenase, 42.0, ferritin, 63.0, and  $\beta$ -galactosidase, 68.6 (23, 48). Except where drawn, the associated error bars were smaller than the symbol dimensions. The arrow corresponds to the observed elution of the  $\beta_1$  gap junction oligomers characterized in later studies as being a hexameric hemi-channel.

be directly compared by CD spectroscopy, since the lipid and detergent molecules are not optically active in the low UV range. Artifacts caused by differential scattering (38) and absorption flattening (39) have been shown to be negligible in sonicated gap junction plaques (22). Contamination of the samples by collagen was corrected by subtraction of the calculated spectral contribution of collagen to the samples (22). No collagen was detected in the samples of isolated solubilized oli-

TABLE I  
Physical characteristics of solubilized oligomers

Stokes radius, $R_s$ (Å)	$41.0 \pm 0.6$
Partial specific volume of complex, $v$ (ml/g)	$0.805 \pm 0.023$
Sedimentation coefficient, $s_{20,w}$ (s <sup>-13</sup> )	$8.76 \pm 0.32$
Molecular mass of complex (kDa)	$208 \pm 5$
Calculated partial specific volume of $\beta_1$ connexin (ml/g)	0.748
Fractional composition (protein)	$0.844 \pm 0.24$
Molecular mass of protein (kDa)	$175 \pm 5$
Frictional ratio, $f/f_{min}$	$1.15 \pm 0.03$

gomers, but the junction membrane samples contained 2.4–3.7% collagen and were corrected by subtracting the spectral contribution of this contaminant.

For soluble proteins, the  $\alpha$ -helix content calculated from the CD spectrum using a non-linear least-squares fitting of the reference data set (29) has been shown to strongly correlate with the helical content as determined by x-ray crystallography. This type of analysis has also been successful in describing the helix content of two membrane-associated polypeptides, bacteriorhodopsin (40) and crambin (41). The discussion of the experimentally determined secondary structure will focus primarily on the  $\alpha$ -helix content since it is not possible to determine other secondary structures with high reliability by this technique.

The averaged CD spectrum of the isolated oligomers was similar, but not superimposable, to that of the intact gap junction plaques (Fig. 4) and appeared to be relatively red-shifted (e.g. the large positive peak at low wavelength, which is indicative of helix-content, appeared red-shifted 2.0 nm relative to that of the membrane-bound sample). Analysis of the membrane plaques indicated that there was 52%  $\alpha$ -helix content in

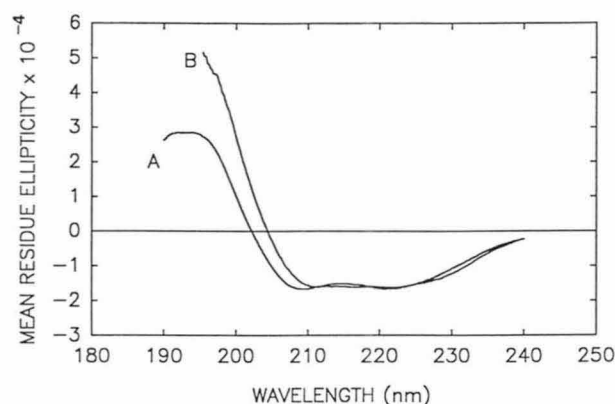


FIG. 4. CD spectra of sonicated gap junction patches (A) and solubilized gap junction complexes (B). The magnitude of the mean residue ellipticity of the spectra were determined using the normalization factor calculated in our analyses.

this protein, consistent with the value determined in previous CD studies (22). The isolated detergent-solubilized oligomers contained 66%  $\alpha$ -helix (Table II).

The extent of agreement between the calculated net structure and the measured CD spectrum is reflected in the NRMSD parameter (42). The NRMSD of the analyzed spectrum of solubilized gap junction complexes was fairly high (0.133). The absorption bands of the spectra of the reference basis set, modeled as Gaussians, were shifted independently to correct for solvent effects, resulting in a substantially improved fit to the experimental data (32). Shifting of the two  $\pi$  to  $\pi^*$  transitions and the single  $n$  to  $\pi^*$  transitions of the reference basis spectra by  $-5$ ,  $0$ , and  $-3$   $\text{mm}^{-1}$ , respectively, lowered the NRMSD to 0.074 in the case of detergent solubilized gap junctions, but did not appreciably affect the calculated secondary structure (67%  $\alpha$ -helix). This type of analysis did not improve the fit for the membrane bound samples (NRMSD = 0.025).

**Chemical Cross-linking**—The oligomeric state of an aggregate may be examined using chemical cross-linking agents to identify the statistical distribution of neighboring molecules. DMS, a membrane permeant, homobifunctional 11-Å linker which reacts with primary amines, has been shown to effectively cross-link large globular oligomers in solution (43) and in membranes (44). The gap junction plaques, resuspended in TEA buffer at pH 9.2, were cross-linked by DMS. Even at reaction times as short as 1 min, these samples were so extensively cross-linked that they failed to enter an 8% SDS-polyacrylamide gel (data not shown). This is probably due to the close proximity of the individual hexamers within a gap junction plaque. However, upon incubation of isolated gap junction oligomers with this cross-linker,  $\beta_1$  protein in higher molecular weight aggregates was detected by immunoblotting. Regularly spaced bands representing the gap junction monomer and oligomers (dimer, trimer, . . . ) up to and including the hexamer were observed, as well as higher order multimers corresponding to cross-linked hexamers (Fig. 5A). The assignment of oligomer stoichiometry was confirmed by the linearity of the semilogarithmic plot of aggregation state versus electrophoretic mobility of the species (Fig. 5B). Assuming that each species is comprised of integral multiples of the  $\beta_1$  polypeptide, the correlation coefficient was closest to unity when the major bands were assigned as being oligomers of 1, 2, 3, 4, 6, 12, and 18 units. Pentameric assemblies were observed in overloaded gels before cross-linking (lane 3), but could not be resolved in lanes containing cross-linked samples due to the high density of observed hexamers (lane 4). The higher order aggregates observed at longer reaction time had molecular weights consistent with those of cross-linked hexamers (12- and 18-mers).

TABLE II  
Calculated secondary structure of gap junction samples

	% Secondary structure	
	$\alpha$ -Helix	NRMSD
Solubilized hexamers	66	0.133
Membrane plaques	52	0.025

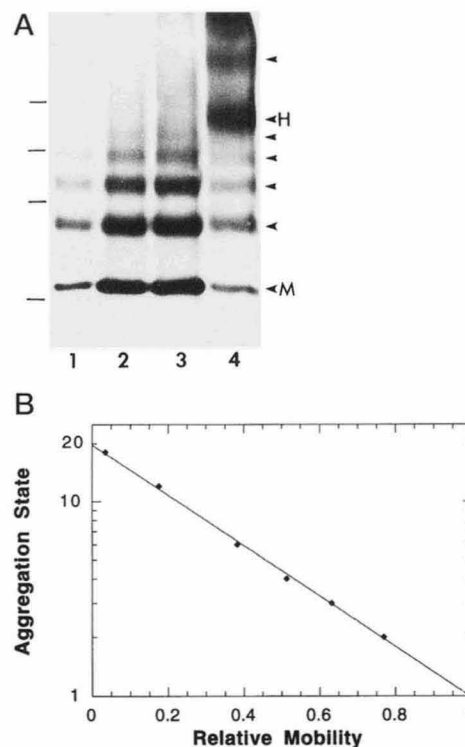


FIG. 5. Chemical cross-linking of Gap junction oligomers. A, immunoblot of cross-linked  $\beta_1$  gap junction oligomers. Samples were applied to a gradient 4–15% SDS-polyacrylamide gel, transferred to nitrocellulose, and treated with antibodies to  $\beta_1$  rat liver connexin. Samples were treated as follows: lane 1, untreated sample (enriched membranes); lane 2, detergent-solubilized sample; lane 3, detergent solubilized samples, preincubated with excess glycine prior to cross-linking with 10 mM DMS; lane 4, detergent-solubilized sample cross-linked with 10 mM DMS. The reaction was quenched with excess glycine after 20 h. The arrowheads on the right side from bottom to top, indicate position of monomers, dimers, trimers, tetramers, pentamers, and hexamers. The lines on the left side indicate the position of molecular mass markers from top to bottom: 205, 116.5, 80, and 32.5 kDa. The positions of the  $\beta_1$  monomer and hexamer are denoted by the letters on the right side by M and H, respectively. B, semilogarithmic plot of aggregation state versus mobility. Lane 4 of A was densitized; a linear relationship was observed for ( $r = 0.9995$ ) with the peak densities corresponding to monomers, dimers, trimers, tetramers, hexamers, dodecamers, and 18-mers.

## DISCUSSION

In this study, gap junction oligomers (connexons) were isolated from enriched rat liver gap junctions by treatment with non-ionic detergent, high pH, and high salt under reducing conditions. These oligomers were then physically characterized as being principally a  $\beta_1$  hexamer with properties equivalent to a single membrane hemi-channel. Immunoblots of eluant from HPLC indicated that the  $\beta_1$  gap junction protein is present in a number of fractions (data not shown, but the  $\beta_1$  elution profile is similar to that observed in FPLC, shown in Fig. 2). However, the concentration of this protein is greatest in the eluant fraction which subsequent studies characterized as having physical parameters consistent with a hexamer. Some gap junction protein also elutes with the void volume as partially solubilized membrane patches or large micelles (observed in micrographs as double membranes and amorphous blobs, and present at

greater concentration when the DTT was not fresh), or as paired hexamers at slightly later volumes (also seen as "doughnuts" in micrographs, data not shown). Immunoblots indicate that  $\beta_1$  protein is also present at higher  $V_e$ , presumably as lower order aggregates (e.g. monomers, dimers, and trimers). Samples prepared for injection contained primarily  $\beta_1$  protein, but a small amount of  $\beta_2$  protein was also present. In FPLC eluant, the  $\beta_2$  protein was observed to co-elute with the  $\beta_1$  species, suggesting a close association between  $\beta_1$  and  $\beta_2$  connexins, since the calculated molecular mass of a  $\beta_1$  hexamer is different from a  $\beta_2$  hexamer (192 versus 156 kDa).

The 6-fold symmetry observed in x-ray diffraction studies (21) and image analysis (17, 19), suggests that the hemi-channel is hexameric. Incubation of the isolated complexes with DMS yielded increasing higher order cross-linked  $\beta_1$  oligomers with time. The molecularity of the reaction products increased step-wise to six, and higher order aggregates were multiples of this hexameric unit (i.e. 12-, 18-, and 24-mers) (Fig. 5). It is possible upon cross-linking of native channels, the pentameric units have shifted molecular weights, such that the dominant band in lane 4 of Fig. 5A corresponds to pentameric units. We think this unlikely since the lower order aggregates (i.e. dimers, trimers, and tetramers) run equivalently independent of cross-linking and their mobility is consistent with the linear regression analysis. Parallel experiments using membrane-bound samples yielded aggregates which did not enter the resolving gel, probably due to extensive cross-linking of the close-packed oligomers.

In the hydrodynamic studies, the calculated size of the isolated oligomer was also consistent with it being a hexamer similar in shape to that of the hemi-channel. Previous x-ray diffraction studies of gap junctions determined that each hexameric channel extends  $\sim 90$  Å from the center of the gap, and it has a radial diameter of  $\sim 50$  Å within the bilayer and  $\sim 60$  Å on either face (the cytoplasmic domain may also project an additional 20 Å onto the membrane plane) (45). Gel filtration studies indicate that the Stokes radius of the solubilized hexamer is  $41.0 \pm 0.6$  Å, which is consistent with these channel dimensions (45). The molecular mass for the complex was determined to be 208 kDa. This calculated mass is the sum of the contributions of protein and detergent in the complex. The calculated  $R_g$ , which is consistent with the channel dimensions, suggests that detergent binding was not extensive. Given that the  $\nu$  of  $\beta_1$  gap junction as calculated from its amino acid composition is 0.748 (proteins typically have  $\nu$  of 0.72–0.76), and LDAO has a  $\nu$  of 1.112, it is calculated that  $\sim 85\%$  of the mass ratio in the protein-detergent complex was due to the protein, and hence the calculated molecular mass for the connexin oligomer is 175 kDa. This must be considered an estimate, since it is critically dependent on determination of  $\nu$  for both detergent-bound and detergent free  $\beta_1$  connexin. Given that the gap junction  $\beta_1$  polypeptide has properties which cause it to run anomalously on SDS-PAGE as a 26–28 kDa band, our calculated molecular mass (which, like SDS-PAGE, is a function of  $R_g$ ) of 175 kDa is consistent with a hexameric assembly of these units.

There are some differences in the secondary structure of the solubilized and "native" gap junction proteins. CD spectroscopic studies indicate that the solubilized gap junction protein is slightly enriched in  $\alpha$ -helix (66% relative to 52% in the membrane bound form). A possible source for this difference may be the partial refolding of the cytoplasmic domain, which has been shown to be sensitive to detergent or alkali treatment (22). Alternatively, the exposed extramembranous domain of the solubilized hexamer may be folded differently than this domain in the membrane-bound samples, which are paired and not exposed to solvent. It is also possible that some of the differences may be attributed to the presence of contaminating species in our membrane preparations, which are removed by

subsequent solubilization and purification. However, the elevated  $\alpha$ -helix content in both samples is more than sufficient for the transmembrane domains to be modeled as  $\alpha$ -helical bundles (14, 45–47).

In summary, these results indicate that the  $\beta_1$ -gap junction protein from rat liver in detergent solution exists as a hexamer and/or multiple of this basic unit. Whether other connexins also exist as a hexamer is not known. However, based on the predicted common topology of the connexin proteins, it is likely that all gap junction proteins exist as hexamers. As shown in this study, both  $\beta_1$  and  $\beta_2$ -connexin co-elute suggesting that they may be associated with each other. However, further experiments will be required to distinguish between heterotypic and heteromeric associations.

**Acknowledgments**—We are grateful to Jessica van Leeuwen for excellent technical assistance, Larry Xue at the Center for Statistics at the University of Pittsburgh for help with the error analysis, and Mark Yeager for helpful discussions throughout the study.

## REFERENCES

- Loewenstein, W. R. (1987) *Cell* **48**, 725–726
- Warner, A. (1992) *Semin. Cell Biol.* **3**, 81–91
- Beyer, E. C. (1993) *Int. Rev. Cytol.* **137C**, 1–37
- Kumar, N. M., and Gilula, N. B. (1992) *Semin. Cell Biol.* **3**, 3–16
- Goodenough, D. A., and Stoekenius, W. (1972) *J. Cell Biol.* **54**, 646–656
- Hertzberg, E. L., and Gilula, N. B. (1979) *J. Biol. Chem.* **254**, 2138–2147
- Hertzberg, E. L. (1984) *J. Biol. Chem.* **259**, 9936–9943
- Nicholson, B., Dermietzel, R., Teplow, D., Willecke, K., and Revel, J.-P. (1987) *Nature* **329**, 732–734
- Paul, D. L. (1986) *J. Cell Biol.* **103**, 123–134
- Kumar, N. M., and Gilula, N. B. (1986) *J. Cell Biol.* **103**, 767–776
- Zhang, J. T., and Nicholson, B. J. (1989) *J. Cell Biol.* **109**, 3391–3401
- Young, J. D., Cohn, Z. A., and Gilula, N. B. (1987) *Cell* **48**, 733–743
- Zimmer, D. B., Green, C. R., Evans, W. H., and Gilula, N. B. (1987) *J. Biol. Chem.* **262**, 7751–7763
- Milks, L. C., Kumar, N. M., Houghten, R., Unwin, N., and Gilula, N. B. (1988) *EMBO J.* **7**, 2967–2975
- Hertzberg, E. L., Disher, R. M., Tiller, A. A., Zhou, Y., and Cook, R. G. (1988) *J. Biol. Chem.* **263**, 19105–19111
- Goodenough, D. A., Paul, D. L., and Jesaitis, L. (1988) *J. Cell Biol.* **107**, 1817–1824
- Unwin, P. N. T., and Zampighi, G. (1980) *Nature* **283**, 545–549
- Unwin, P. N. T., and Ennis, P. D., (1984) *Nature* **307**, 609–613
- Stauffer, K. A., Kumar, N. M., Gilula, N. B., and Unwin, N. (1991) *J. Cell Biol.* **115**, 141–150
- Caspar, D. L. D., Goodenough, D. A., Makowski, L., and Phillips W. C. (1977) *J. Cell Biol.* **74**, 605–628
- Makowski, L., Caspar, D. L. D., Phillips, W. C., and Goodenough, D. A. (1977) *J. Cell Biol.* **74**, 629–645
- Cascio, M., Gogol, E., and Wallace, B. A. (1990) *J. Biol. Chem.* **265**, 2358–2364
- le Maire, M., Aggerbeck, L. P., Monteilhet, C., Andersen, J. P., and Møller, J. V. (1986) *Anal. Biochem.* **154**, 525–535
- Laemmli, U. K. (1970) *Nature* **224**, 149–154
- Risek, B., Guthrie, S., Kumar, N. M., and Gilula, N. B. (1990) *J. Cell Biol.* **110**, 269–282
- Towbin, H., Staehelin, T., and Gordon, J. (1979) *Proc. Natl. Acad. Sci. U. S. A.* **76**, 4350–4354
- Savitzky, A., and Golay, M. J. E. (1964) *Anal. Chem.* **36**, 1627–1639
- Mao, D., Wachter, E., and Wallace, B. A. (1982) *Biochemistry* **21**, 4960–4968
- Chang, C. T., Wu, C. C., and Yang, J. T. (1978) *Anal. Biochem.* **91**, 13–31
- Cascio, M., and Wallace, B. A. (1994) *Protein Peptide Lett.* **1**, 136–140
- Cascio, M., and Wallace, B. A. (1988) *Proteins* **4**, 89–99
- Cascio, M., and Wallace, B. A. (1995) *Anal. Biochem.* **227**, 90–100
- Ackers, G. K. (1967) *J. Biol. Chem.* **242**, 3237–3238
- le Maire, M., Ghazi, A., Martin, M., and Brochard, F. (1989) *J. Biochem. (Tokyo)* **106**, 814–817
- Clarke, S. (1975) *J. Biol. Chem.* **250**, 5459–5469
- Clarke, S., and Smigel, M. D. (1989) *Methods Enzymol.* **172**, 696–709
- Reynolds, J. A., and McCaslin, D. R. (1985) *Methods Enzymol.* **117**, 41–53
- Schneider, A. S., and Harmatz, D. (1976) *Biochemistry* **15**, 4158–4162
- Gordon, D. J., and Holzworth, G. (1971) *Arch. Biochem. Biophys.* **142**, 481–488
- Mao, D., and Wallace, B. A. (1984) *Biochemistry* **23**, 2667–2673
- Wallace, B. A., Kohl, N., and Teeter, M. M. (1984) *Proc. Natl. Acad. Sci. U. S. A.* **81**, 1406–1410
- Brahms, S., and Brahms, J. (1980) *J. Mol. Biol.* **138**, 149–178
- Lee, L., Kelly, R. E., Pastra-Landis, S. C., and Evans, D. R. (1985) *Proc. Natl. Acad. Sci. U. S. A.* **82**, 6802–6806
- Smith, A. P., and Loh, H. H. (1978) *Biochemistry* **17**, 1761–1765
- Makowski, L., Caspar, D. L. D., Phillips, W. C., and Goodenough, D. A. (1984) *J. Mol. Biol.* **174**, 449–481
- Unwin, N. (1989) *Neuron* **3**, 665–676
- Tibbitts, T. T., Caspar, D. L. D., Phillips, W. C., and Goodenough, D. A. (1990) *Biophys. J.* **57**, 1025–1036
- Sadler, J. E., Rearick, J. I., Paulson, J. C., and Hill, R. L. (1979) *J. Biol. Chem.* **254**, 4434–4443